Insights into the Reactions of Hydroxyl Radical with Diolefins from Atmospheric to Combustion Environments

Fethi Khaled, Binod Raj Giri, Dapeng Liu, Emmanuel Assaf, Christa Fittschen, Aamir Farooq

Insights into the Reactions of Hydroxyl Radical with Diolefins

Fethi Khaled[1], Binod Raj Giri[1], Dapeng Liu[1], Emmanuel Assaf[2] , Christa Fittschen[2], Aamir Farooq[1]

[1]King Abdullah University of Science and Technology, Clean Combustion Research Center, Physical Sciences and Engineering Division, Thuwal 23955-6900, Saudi Arabia

[2]Université Lille, CNRS, UMR 8522 - PC2A - Physicochimie des Processus de Combustion et de l'Atmosphère, F-59000 Lille, France

Abstract

Hydroxyl radicals and olefins are quite important from combustion and atmospheric chemistry standpoint. Large amounts of olefinic compounds are emitted into the earth's atmosphere from both biogenic and anthropogenic sources. Olefins also make a significant share in the tranportation fuels (e.g., 10 – 15% in gasolines), and they appear as important intermediates during hydrocarbon oxidation. As olefins inhibit low-temperature heat release, they have caught some attention for their applicability in future advanced combustion engine technology. Despite their importance, the literature data for the reactions of olefins are quite scarce. In this work, we have measured the rate coefficients for the reaction of hydroxyl radicals (OH) with several diolefins, namely 1,3-butadienes, *cis*-1,3-pentadiene, *trans*-1,3-pentadiene, and 1,4-pentadiene, over a wide range of experimental conditions (T = 294 – 468 K and p ~ 0.048 bar; T = 881 – 1348 K and p ~ 1.5 bar). We obtained the low-T data in a flow reactor using laser flash photolysis and laser induced fluorescence (LPFR/LIF), and the high-T data were obtained with a shock tube and UV laser-absorption (ST/LA). At low temperatures, we observed differences in the reactivity of *cis*- and *trans*-1,3-pentadiene, but these molecules exhibited similar reactivity at high temperatures. Similar to monoolefins + OH reactions, we observed negative temperature dependence for dienes + OH reactions at low temperatures – revealing that OH-addition channels prevail at low temperatures. Except for 1,4-pentadiene + OH reaction, other diolefins studied here almost exclusively undergo addition reaction with OH radicals at the low-temperature end of our experiments, whereas the reactions mainly switch to hydrogen abstraction at high temperatures. These reactions show complex Arrhenius behaviour for the temperature depedance as a result of many possible chemical processes in such a convoluted system.

1. Introduction

Global demands for petroleum-based liquid fuels is increasing at an average annual rate of ~1%[1] as the transport sector is almost entirely powered by internal combustion engines (ICEs) burning these fuels. The current scenario of renewable sources makes a slim outlook to surpass petroleum-based fuel in the forseeable future, and the share of renewables will likely make up only ~ 10% even by 2040. Hence, ICEs will continue to power transport sectors to a large extent for decades to come. Curbing of environmental pollution and greenhouse gas emissions will thus remain a big challenge. At the present time, it seems that the best way to mitigate harmful impacts of transport system is to improve the combustion technology, e.g., by developing new fuel-engine systems. Lately, there has been a lot of interest on fuel-engine design optimization due to stringent emission restrictions and efficiency considerations worldwide.[2-67] The aim of such studies is to optimize the fuel properties for the best performance in advanced low-temperature combustion modes.

Octane sensitivity (OS) of a fuel is an important metric for fuel-engine correlation which measures how differently a fuel responds to changing conditions such as intake temperature, intake pressure and compression ratio. OS is defined as the difference between research octane number (RON) and motor octane number (MON), i.e., OS = RON – MON. Kalghatgi[2, 4] proposed another metric, called the Octane Index (OI), to better characterize the antiknock property of a fuel. OI is given by OI = RON – K*OS, where K is an empirical parameter determined experimentally in engines. As K is negative for most modern engines, a fuel with higher OS gives larger value of OI, and thereby it may allow an engine to operate more efficiently.[2, 4] Current trends in the development of more efficient spark ignition (SI) engines are towards increasing the compression ratios and implementing turbocharging.[4] The challenge is that it may cause engine knocking as ignition delay times drop sharply with increasing cylinder

pressure. As ignition delay times of high OS fuels tend to decrease less rapidly with increasing pressure, smaller chain olefinic fuels may provide the desired antiknock quality. Unlike most paraffins, olefins have relatively high octane sensitivity due to the presence of double bond(s), e.g., 1-butene (OS = 15.7), 2-ethyl-1-butene (OS = 18.9), and 1-pentene (OS = 12.9) have much higher OS than *n*-butane (OS = 4) and *n*-heptane (OS = 0).[8] These small chain olefinic fuels do not exhibit "cool flames" or negative temperature coefficient (NTC) behavior due to the lack of low-temperature reactivity. Leppard[9] and Westbrook et al.[8, 10] have discussed the connection between octane sensitivity of olefinic hydrocarbon fuels and the lack of low-temperature reactivity. Basically, the inhibition of low-temperature reactivity of these olefins may be attributed to the production of highly stable allylic type of radicals (resonance energy of ~60 kJ/mol for unconjugated and $\geq$ 80 kJ/mol for conjugated allyls)[11] following hydrogen abstraction from the reactive allylic sites of olefins.

A significant amount of olefins, as high as 15 – 20%,[10] is present in gasolines. They are also found in other transportation fuels like aviation and diesel fuels. These olefins contribute substantially to the octane rating and hence determine the ignition behavior of the fuel. Likewise, the degree of unsaturation in biodiesels greatly affects their cetane quality, ignition delay times and CO/HC emission.[12] Olefins also appear as important intermediates during hydrocarbon oxidation processes. From combustion prospectives, dienes (C_nH_{2n-2}) are particularly interesting because of the presence of two double bonds. The location of the double bonds (conjugated or not) and the number and type of available allylic hydrogens alter the reactivity of olefinic molecules. For example, 1,3-butadiene is the simplest conjugated diene which reacts with OH radicals by roughly three times slower than that of 1-butene near 1200 K.[13-15] 1,3-Butadiene builds up to a significant concentration during combustion of hydrocarbon fuels.[16] Dienes

contribute to the formation of benzene, a soot precursor, and hence the chemistry of dienes governs the kinetics of soot formation processes.[16, 17]

Kinetic studies about the combustion behavior of dienes are quite scarce in the literature. Most of the earlier studies were carried out near ambient temperatures.[18-25] At higher temperatures, only 1,3-butadiene caught the attention of most researchers.[13, 26, 27] Li et al.[26] measured ignition delay times of 1,3-butadiene in a shock tube and a rapid compression machine. Not surprisingly, they observed a clear lack of NTC region due to the suppression of low-temperature reactivity of 1,3 butadiene. Li et al.[28] measured the rate coefficients for the reaction of 1,3-butadiene + OH at T = 240 – 340 K and p ~ 1 Torr in a discharge flow reactor using relative rate method. Their measured rate coefficients exhibited negative temperature dependence given by the Arrhenius expression $k\,(T) = (1.58 \pm 0.07) \times 10^{-11} \exp[(436 \pm 13)/T]$ cm^3 molecule^{-1} s^{-1}. In another work, Li et al.[27] performed a detailed theoretical analysis of H + 1,3-butadiene reaction over a wide range of pressure and temperature. They found that H addition preferentially occurs (> 80%) at the terminal carbon atom at all temperatures (T = 298 – 2000 K), whereas abstraction of H atom from the central carbon atom is the dominant channel contributing more than 70% at all temperatures. Vasu et al.[13] measured the rate coefficients of 1,3-butadiene + OH reaction over T = 1011 − 1406 K and p ~ 2.2 bar using shock tube and laser absorption technique. Additionally, they performed variational transition-state theory using the parameters obtained from QCISD(T)/cc-pVT∞Z//B3LYP/6-311++G(d,p) level of theory to rationalize terminal vs. non-terminal H atom abstraction. Their total abstraction rate coefficients beyond 1200 K agreed very well with the experimentally determined values. However, their theoretical values systematically underpredicted the measured rate coefficients below 1200 K. They reasoned this to the opening of a new reaction channel at lower temperatures, *i.e.,* addition of OH to the double bond of 1,3-butadiene. This indicates that unlike monoalkenes + OH, addition of OH to dienes — depending upon the degree of conjugation — can prevail at relatively higher temperatures. Therefore,

dienes + OH are expected to show a complex nature of temperature and pressure dependence of the rate coefficients due to the many competing channels (addition, abstraction, back-dissociation, isomerization and bimolecular). This warrants additional chemical kinetic studies beyond this simplest conjugated diene (1,3-butadiene) to better characterize the reactions of dienes with OH radicals.

Olefins are not only important in combustion but also in atmospheric chemistry. Large amount of these compounds is emitted into the earth's atmosphere from both biogenic and anthropogenic sources, e.g., automobile emissions, evaporation of transportation fuels, tobacco smokes, forest fires, biogenic isoprenes and terpenes.[29-31] OH initiated oxidation of olefins is one of the main pathways for the fate of these hydrocarbons in the atmosphere.[25] The atmospheric chemistry of polyolefins are more interesting as they offer more reaction pathways with OH radicals giving rise to larger rate constants than that of monoolefins. Reactivity of a hydrocarbon with OH radicals in the atmosphere also affects the formation of ozone. Peeters et al. [23] recently developed an approach based on structure-activity relationship (SAR) to discern the site-specific addition of OH radicals to the double bond(s) of olefins at 298 K. Their site-specific SAR approach provided excellent predictive capabilities for the site-specific and total rate coefficients for 65 OH + (poly)olefin reactions with an uncertainty of ~ 15%. From their detailed analysis, they showed that the total rate coefficients of OH + (poly)olefins reactions may be accurately estimated by adding the individual rate coefficients for the addition of OH radicals to the specific carbon-carbon double bond(s) of (poly)olefin. Furthermore, they stated that this simple approach of summing up of site-specific OH-addition rate coefficients is not valid for some compounds like α-terpinene and α-phelandrene because significant contributions come from the abstraction of H atoms in such molecules. For the reactions of α-terpinene and α-phelandrene with OH radicals, the deviations in their SAR predicated values were as large as 40%. Ohta[18] determined

rate coefficients for 19 diolefin + OH reactions at ambient conditions utilizing relative rate method. Not surprisingly, they observed an increase in the rate coefficients for diolefins + OH reaction with the increase of alkyl substituents on the double bond(s). They showed that the reactivity of OH radicals with diolefins, except allenes and cyclic diolefins, may be accurately estimated by summing up the rate coefficient contributions from individual carbon-carbon double bonds. However, they had to multiply the rate coefficients of analogous monoolefin by a factor of 1.24 to estimate the rate coefficients for conjugated olefins + OH reactions. Ohta attributes this multiplication factor to the resonance effect that promotes the addition of OH radicals to conjugated dienes.There are other SAR approaches[18, 21, 24, 25, 32-34] of varying degrees of accuracy in the literature.

From the discussion above, it is seen that OH + diolefins display very interesting chemistry, and that there are limited literature data available in quite narrow thermodynamic conditions. Our current knowledge of these reactions is not adequate for the development of robust combustion and atmospheric models. Therefore, in the current work, we aim to provide new insights for OH + diolefins reactions by determining the rate coefficients of OH radicals with conjugated-π systems like 1,3-butadiene, *trans*- and *cis*-1,3-pentadiene, and non-conjugated-π system like 1,4-pentadiene. The trends observed will be discussed and analyzed to rationalize the reactivity of diolefins with OH radicals.

2. Experimental Method

We investigated the reactions of OH radicals with 1,3-butadiene (1,3-C_4H_6, R1), stereo-isomers of 1,3-pentadiene (*cis*-1,3-C_5H_8, R2; *trans*-1,3-C_5H_8, R3) and 1,4-pentadiene (1,4-C_5H_8, R4) over a wide range of experimental conditions using a low-pressure shock tube facility (T = 881 –

1348 K, p ~ 1 – 2.5 bar) at King Abdullah University of Science and Technology (KAUST) and a laser photolysis flow reactor (T = 291 – 468 K, p ~ 40 mbar) at University of Lille.

1,3-C_4H_6 + OH → products (R1)

cis-1,3-C_5H_8 + OH → products (R2)

trans-1,3-C_5H_8 + OH → products (R3)

1,4-C_5H_8 + OH → products (R4)

Shock Tube/Laser Absorption (ST/LA): As the details of the ST/LA technique are provided in our earlier works [35], here, we describe the experimental setup very briefly. The stainless steel shock tube has an inner diameter of 14.2 cm, and consists of a 9 m long driven section and a variable length driver section. For this work, we used a 3 m long driver section to achieve an adequate reaction time of ~1.5 ms behind reflected shock waves. We used a polycarbonate diaphragm of thickness 5 mm to separate the driven section from the driver section and to achieve reflected shock pressure of ~1.5 atm. We generated shock waves by pressure bursting of the diaphragm. The shock wave propagated into the driven section, heating and pressurizing the test gas mixture almost instantenously. We employed a series of five PCB 113B26 piezoelectric pressure transducers, placed in the last 1.3 m of the driven section, to measure the incident shock speed. We used the shock speed and initial temperature / pressure of the shock tube to calculate the temperature and pressure behind the reflected shock wave. For these calculations, we used the Frosh code [36] which is based on shock-jump relations [37].

We used a narrow-width Spectra-physics dye laser system to generate ultra-violet (UV) light near ~307 nm. We achieved a UV light beam of 307 nm by the external frequency doubling of red light (614 nm), produced by a ring-dye cw laser, which is pumped at 532 nm by a solid state

Nd:YAG laser. We tuned the UV light precisely to the center (306.6868 nm) of the well-characterized R1(5) line in the (0, 0) absorption band of the $A^2\,\Sigma^+ \leftarrow X^2\,\Pi$ electronic transition of OH radical. We used two quartz optical windows at 2 cm away from the endwall to guide UV light beam into the reaction zone of the shock tube for OH detection. We chose *tert*-butyl hydroperoxide (TBHP) for OH radical source as it decomposes very rapidly (half-life ≤ 5 μs for T > 800 K) to generate OH and $(CH_3)_3CO$ radicals.[38] We employed two modified Thorlab PDA36-EC photodetectors to measure the laser intensity before and after the shock tube. The noise of the laser beam after common-mode-rejection was lower than 0.1% of the signal. Using Beer-Lambert law, absorbance (A) = $\ln(I_0/I) = X_{OH}k_{OH}PL$, we quantitatively converted laser-intensity time profile into OH mole fraction (X_{OH}) time profile. Here, I and I_o are the transmitted and incident laser intensities, k_{OH} stands for the OH-absorption coefficient at 306.68 nm, P and L are the total pressure and the optical path-length (14.2 cm), respectively.

Laser Photolysis Flow Reactor/Laser Induced Fluoresence (LPFR/LIF): Low-temperature experiments for the reactions of OH radicals with dienes were carried out using LPFR/LIF technique; the details of which can be found elsewhere.[39,40, 41] Here, only a brief description is given. The flow reactor is a stainless steel cell that is equipped with external heating coil. Temperatures up to 500 K are attainable inside the reactor, and the temperature at the center of the reactor is read using a fast response thermocouple within an uncertainty of 1 K. The photolysis beam enters the long axis of the flow reactor *via* a quartz window and generates OH radicals after laser flash photolysis of H_2O_2 at 248 nm. The photolysis laser beam was produced by an excimer laser (Lambda Physik LPX 201) operating at a repetition rate of 1 Hz and a laser fluence of ~70 mJ cm^{-2}. This repetition rate ensured an adequate time for the complete replenishment of the gasous mixtures inside the flow reactor between successive laser photolysis pulses. Furthermore, photolysis beam intensity was checked at both the entrance and

the exit of the flow reactor to ensure spatial uniformity of OH radical concentration. For OH excitation, the probe laser beam was introduced through the short axis of the reactor, perpendicular to the photolysis beam. The probe laser light at 282 nm was produced by frequency doubling of a dye laser (Sirah Laser PrecisionScan PRSC-24-HPR, rhodamine 6G dye). This dye laser was pumped by the frequency-doubled output of an Nd:YVO_4 laser (Spectra Physics Navigator II YHP40-532QW). The probe laser has an output beam power of ~35 mW and a repetition rate of 10 kHz. The synchronisation between the photolysis and probe beam was controlled with the help of a delay generator (Princeton Research 9650).

Hydroxyl radical excitation at 282 nm corresponds to the (1,0) vibrational band of the A-X electronic transition. Following OH radical excitations at 282 nm, OH radical decay was monitored by capturing the laser induced fluorescence (LIF) signals leaking out of the axis perpendicular to both the photolysis and probe beam. The red-shifted fluorescence signals were detected at ~308 nm by a photomultiplier (Hamamatsu R212) after passing through an interference filter (308 ± 10 nm). As the excitation laser was operated at 10 kHz giving data point every 100 μs, the LIF signal was acquired for 1 s corresponding to 10,000 data points, i.e., 5000 data points were recorded before each photolysis pulse to measure the background signal and 5000 data points after the photolysis pulse. Each data point was summed over ~100 photolysis pulses. The details of synchronization of various units and data acquisition can be found elsewhere.[39,40, 41]

Chemicals and Mixture Composition: We purchased 1,3-butadiene (99% purity), 1,4-pentadiene (99%), and *tert*-butyl-hydroperoxide aqueous solution (TBHP, 30% solution in water) from Sigma Aldrich, whereas *cis*-1,3-pentadiene (89% purity) and *trans*-1,3-pentadiene (95% purity) were purchased from ChemSampCo. As per vendors data sheet, the main impurities

of *cis*-1,3-pentadiene are t*rans*-1,3-pentadiene (1.79%), 2-methyl-2-butene (0.44%), cyclopentene (0.61%) and cyclopentane (8.36%). *Trans*-1,3-pentadiene contained cyclopentane (3.2%) and *cis*-1,3-pentadiene (1.8%) as impurities. We obtained argon and helium from AH Gases, and their purity was 99.999%. For ST/LA experiments, we prepared gas mixtures, diluted in argon, manometrically in a 24-litre teflon-coated stainless-steel vessel equipped with a magnetically-driven stirrer. The mixtures were left to homogenize for at least one hour. As for LPFR/LIF experiments, dilute mixtures of dienes in helium were prepared in a glass bulb. Prior to preparation of gas mixtures, the mixing vessel or glass bulb was turbo-pumped down to $<10^{-5}$ Torr. Table 1 compiles the mixture compositions used in this work.

Table 1: Mixture composition for **ST/LA** and **LPFR/LIF** experiments with argon and helium as diluents, respectively.

Reaction system	**ST/LA experiments**		**LPFR/LIF experiments**	
	[Fuel]	[TBHP]	[Fuel]	[H_2O_2]
1,3-butadiene	--	--	15-70 ppm	0.3-3 ppm
cis-1,3-pentadiene	300-400ppm	10-20 ppm	3-30 ppm	0.3-3 ppm
trans-1,3-pentadiene	300-500ppm	10-20 ppm	3-30 ppm	0.3-3 ppm
1,4-pentadiene	--	--	3-30 ppm	0.3-3 ppm

As seen in Table 1, we carried out all experiments with excess concentration of dienes as compared to OH radicals. Under such conditions, one may expect the measured OH decay to follow the first-order kinetics, and the decay of OH radicals will mainly be governed by the reaction under investigation. For ST/LA experiments, we used a ratio for fuel to TBHP of 20 or higher, and for LPFR/LIF experiments, we introduced the dilute mixtures of dienes into the flow

reactor by adding a small flow of the mixture to the main flow of helium through calibrated mass flow controllers. We obtained a variable concentration of water-free H_2O_2 in the flow reactor by adjusting the flow of helium through the flask containing a mixture of urea-H_2O_2 powder and SiO_2 at 40 ^{0}C. We obtained a typical concentration of H_2O_2 ~1×10^{14} cm^{-3} *via* the thermal decomposition of H_2O_2-urea mixture. By adjusting the flow, we were able to determine an optimum working condition that gave us a sufficiently low background signal and a good signal-to-noise ratio for OH traces.

3. Results and discussion

High-Temperature Kinetics. High-temperature data were obtained behind reflected shock waves using ST/LA technique for a wide range of experimental conditions (T = 881 – 1348 K, p ~ 1 – 2.5 bar). Figure 1 displays a representative OH time-history measured at T = 1116 K and p = 1.41 bar for a case of 300 ppm *cis*-1,3-pentadiene, 20 ppm TBHP diluted in argon. The inset Figure 1 illustrates an example of pseudo-first order decay of OH radicals, justifying well-tailored mixture compositions. However, the overall reaction rate coefficiens were obtained from detailed kinetic modeling to account for the contributions from secondary chemistries. Our kinetic model is composed up of sub-mechanism for TBHP chemistry taken from Pang et al. [42] with updates for the sensitive reactions from Badra et al. [43] and Mehl et al.[44] gasoline surrogate mechanism that contains the sub-mechanism for 1,3-pentadiene and 1,4-pentadiene. The best fit to the experimentally measured profiles was obtained by treating the rate coefficient of the target reaction as variable. The red line in Fig. 1 shows an example of such a best fit, and also shown is the effect of ±30% perturbations from the best value (k_2 = 2.45×10^{-11} cm^3 molecule^{-1} s^{-1} at 1116 K, 1.41 bar for R2). Table 1 compiles the current measurements for the overall high-temperature rate coefficients of *cis*-1,3-Pentadiene + OH (R2) and *trans*-1,3-Pentadiene + OH (R3) reactions.

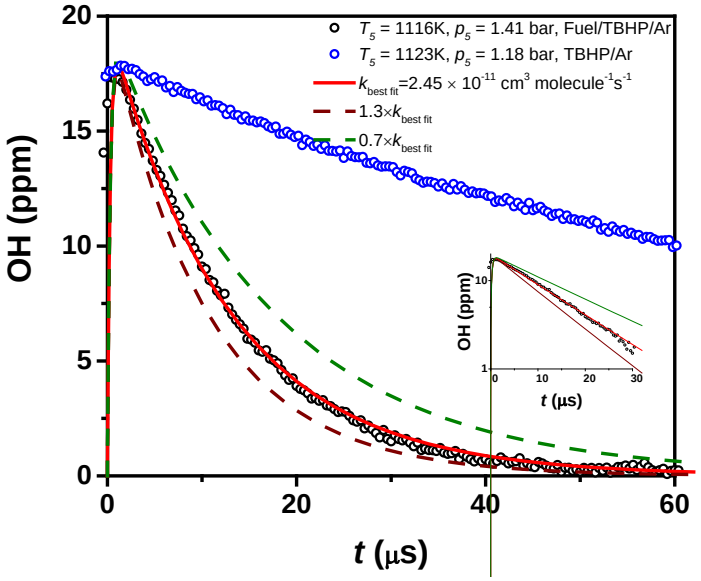

Figure 1: A typical OH time profile measured during OH + *cis*-1,3-pentadiene reaction (R2) using ST/LA technique. Mixture composition: 300 ppm *cis*-1,3-pentadiene, 20 ppm TBHP in argon . The best fit indicated by red line corresponds to a rate coefficients of 2.45×10^{-11} cm^3 molecule^{-1} s^{-1}, dashed lines show a ±30% perturbation from the best value Inset figure shows ln[OH] vs time plot to demonstrate that OH decay obeys the pseudo-first order kinetics. Blue symbols represent a control experiment for OH time history carried out for a mixture of TBHP in argon without fuel.

Table 1: Overall high-temperature rate coefficients for *cis*-1,3-pentadiene + OH (R2) and *trans*-1,3-pentadiene + OH (R3) reactions. The uncertainties in the rate coefficient are +11% / -9% (see Table 2).

***cis*-1,3-pentadiene + OH (R2)**			***trans*-1,3-pentadiene + OH (R3)**		
T (K)	p (bar)	k_2 (10^{-11}cm^3 molecule^{-1} s^{-1})	T (K)	p (bar)	k_3(10^{-11}cm^3 molecule^{-1}s^{-1})
909	1.55	1.78	881	1.36	1.50
918	1.75	1.66	921	1.58	1.80
951	1.33	1.84	936	1.81	1.69
972	1.68	1.73	1006	1.76	1.92
989	1.33	1.89	1025	1.22	1.96
989	1.25	2.03	1034	1.24	2.11
1004	1.15	1.92	1047	1.7	2.14
1024	1.32	2.02	1056	1.28	1.87
1028	1.65	1.82	1059	1.18	2.02
1067	1.59	2.04	1073	1.21	2.05
1110	1.54	2.13	1121	1.78	2.15
1116	1.41	2.45	1139	1.22	2.19
1136	1.2	2.34	1144	1.72	2.20
1166	1.52	2.26	1147	1.23	2.37
1168	1.3	2.42	1159	1.15	2.40

1216	1.36	2.56	1202	1.6	2.18
1236	1.54	2.44	1215	1.17	2.38
1236	1.53	2.44	1245	1.56	2.47
1252	1.14	2.66	1273	1.38	2.64
1282	1.51	2.57	1273	1.46	2.55
1330	1.53	2.92			

We determined uncertainty bounds in our measured rate coefficients by identifying and quantifying various sources of errors. The error sources and the estimated uncertainties in the measured rate coefficients of the targeted reaction are listed in Table 2. While determining the magnitude of each individual error souce, the error source was purturbed to the lower and upper bounds to acquire the best fit to the experimentally measured OH profiles by adjusting the rate coefficient of the target reaction. By doing so, the uncertainties in the rate coefficients from all error sources were quantified at a particular temperature and pressure and later lumped together using the root-mean-square method. We did not incorporate mole fractions of impurity components in our kinetic model to determine their uncertainty contributions to the measured rate coefficients. Instead, we simply estimated the total rate coefficients for OH reactions with the individual impurity components and added these together to get a final value of the rate coefficient that translated into a percentage error in the overall measured rate coefficients. Our estimate suggests that all impurity components present in *cis*-1,3 pentadiene induce 1% and 8% errors in the measured overall rate coefficients at 1000 K and 298 K, respectively; whereas the induced errors for *trans*-1,3 pentadiene is even less, 0.5% and 4%, respectively. The overall uncertainty of the measured rate coefficients for R2 and R3 was found to be +11% / -9% at 1000 K and 1.5 bar.

Table 2: Uncertainty quantification of high-temperature rate coefficients for OH reactions with *cis*-1,3-pentadiene (R2) and *trans*-1,3-pentadiene (R3)

	cis-1,3-pentadiene	*trans*-1,3-pentadiene	*cis*-1,3-pentadiene	*trans*-1,3-pentadiene
Temperature	±2%		2%	
Impurity(%)	±11%	±5%	1%	0.5%
Fuel concentration (%)	±5%		5%	
Fitting procedure	5%		5%	
OH absorption signal noise	3%		1%	
Secondary chemistry	TBHP + OH ⇒ TBUTOXY + OH, ±30% CH_3 + OH ⇒ CH_2 + H_2O, factor of 2		5% for T <1000K, 0.5% for T >1000K 3%	
Others (absorption coefficients, pressure …)			3%	
Root-mean-square error			+11% / -9%	+11% / -9%

Figure 2 displays Arrhenius plots for the overall rate coefficients of reactions R1 – R4 measured in this work along with literature data of straight chain olefins for comparison. As can be seen, these olefins display very interesting reactivity towards OH radicals by exhibiting severe curvature of varying degree for the temperature dependence of the rate cofficients. Such complex Arrhenius behavior, shown by these olefins + OH reactions, is the result of the combined effect stemming from various chemical processes, e.g., abstraction, addition, back dissociation and non-abstraction bimolecular channels. Of course, the complexity of (poly)olefins + OH reactions

depend upon their underlying potential energy surfaces, and the accuracy of the potential energy surfaces will determine the quality of the predicted rate coefficients for these individual chemical processes. As we will discuss low-temperature chemistry in the next section, we focus here on the high-temperature reactivity trends of these olefins (conjugated or unconjugated) with OH radicals to draw some useful conclusions. As stated earlier, there are limited high-temperature literature data for diolefins + OH reactions for meaningful comparision.

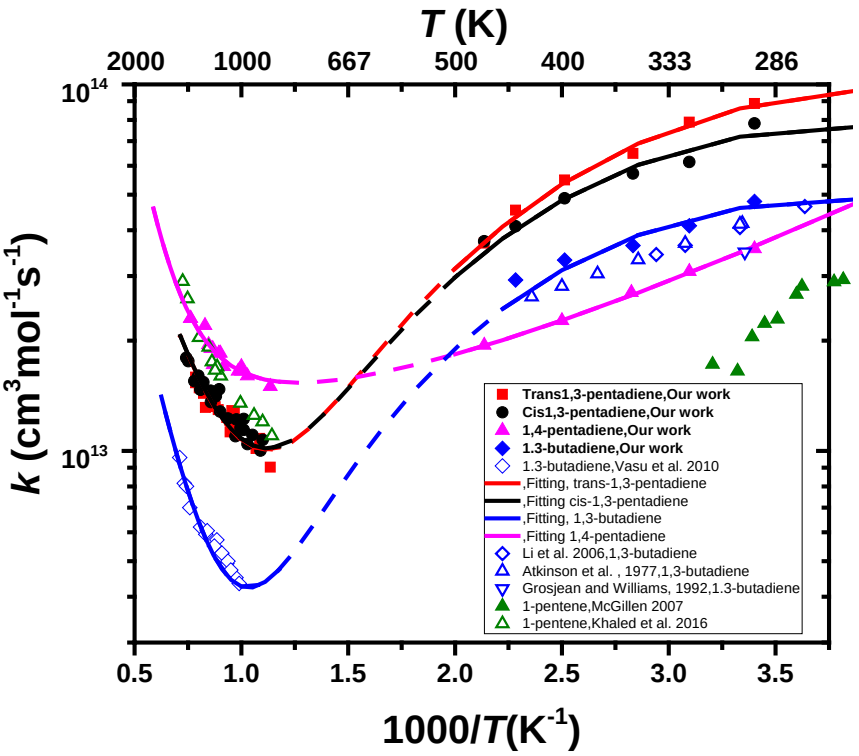

Figure 2: Arrhenius plot for the total rate coefficients of OH radical reactions with 1,3-butadiene (R1), *cis*/*trans*-1,3-pentadiene (R2 and R3) and 1,4-pentadiene (R4) along with selected literature data: 1,3-butadiene [13, 21, 22, 28]; *trans* and *cis*-1,3-pentadiene from Magneron et al. [20]; *cis*-1,3-pentadiene from Ohta et al. [18]; 1,4-pentadiene high temperature data from Giri et al.[45]; 1-pentene from Khaled et al.[15] and McGillen et al. [19]. Lines represent the best fit to the experimental rate coefficients that can be best described by eqs. 1 – 4. Due to the complex nature of these (poly)olefins + OH reactions, the broken lines caution the users for using eqs. 1 – 4 to obtain total rate coefficients in the intermediate temperature region.

First, we notice that both *cis*- and *trans*-1,3 pentadiene exhibit similar reactivity under high-temperature conditions (see Figure 2). This may indicate that these isomers have isomerized

quickly to yield equilibrated population of both conformers before undergoing reaction with OH radicals. Our finding appears to resonate well with the results of Marley et al. [46] who studied the isomerization reaction of *cis*- and *trans*-1,3-pentadiene in the shock tube and reported an isomerization rate expression of $k_{cis \rightarrow trans}=10^{13.6}$ exp(-63000/4.58*T*) s^{-1} resulting in $t_{1/2} \leq 0.5$ μs for $T \geq 800$ K. However, we are not certain about this rate expresssion as the authors are not consistent with their reported values of the Arrhenius parameters. For example, they used A_∞ = 13.6 s^{-1} and E_a = 53.0 kcal/mole in another occasion and stated that the conversion was very small and that they never reached equilibrium in their experiments for the residence time of 150 μs. That being said, *cis*- and *trans*-1,3-pentadiene may not undergo fast isomerization even at high temperatures, and that they would still retain their conformational identity. If it is so, then one would expect *trans*-1,3-pentadiene to react somewhat faster than *cis*-1,3-pentadiene, similar to that observed in the reactions of *cis/trans*-2-pentene and *cis/trans*-2-hexene with OH radicals at high temperatures.[15] But, we do not observe any differences in the reactivity for the plausible reason being that the expected reactivity differences are masked within the reported uncertainty of ±10% of our experiments.

Secondly, we observed that these diolefins + OH reactions exhibit pronounced positive temperature dependence at high temperatures, revealing that these reactions primarily undergo chemical pathways having sizable energy barriers, e.g., hydrogen abstraction and/or non-abstraction bimolecular pathways. The reactions of OH radicals with c*is*- and *trans*-1,3 pentadienes display a weaker *T*-dependance and larger rate coefficients by a factor of ~3 as compared to 1,3-butadiene. Note that both are conjugated diolefins, and that the barrier heights and relative energies of the product radicals, following OH addition to the terminal carbon atom of C=C, are expected to be comparable due to similar resonance energy of the stabilized adduct radicals. This means the contribution of the addition channels in both cases might be of comparable magnitude, and consequently, as the C-H vinylic bond is strong (bond dissociation

energy ≥108 kcal/mole)[47] and their removal *via* abstraction is slow, the difference in the reactivity and temperature dependance comes largely from the abstraction of comparatively loosely bound –CH_3 allylic hydrogens atoms (BDE = 82 – 85 kcal/mole)[47] in *cis*-/*trans*-pentadienes which are absent in 1,3-butadiene. At high temperatures, if we were to estimate the overall rate coefficients by summing up all the site-specific rate coefficients for hydrogen abstractions[13, 48] of 1,3-pentadiene, i.e., $k_{overall}(T) = k_{abstraction}(T) + k_{addition}(T) + k_{non\text{-}abstraction}(T) \approx k_{abstraction}(T) \approx 2\times k_{terminal\ (vinylic)}(T) + 3\times k_{non\text{-}terminal\ (vinylic)}(T) + 3\times k_{allyl}(T)$, we obtain very good match between our experimental data and predicted rate coefficients at the high-temperature end of our experiments. However, the deviations are large at lower temperatures (as large as 30% around 1000 K). At lower temperatures, the predicted rate coefficients systematically underpredict our experimental data. Similar observations were made by Vasu et al.[13] for 1,3-butadiene + OH reaction. At temperatures lower than 1200 K, their measured rate coefficients were larger (~20% at 1000K) than their theoretical predictions. This may allow us to conclude that, for conjugated diolefins + OH reactions, addition and/or non-abstraction bimolecular channels contribute significantly to the overall rate coefficients even at temperatures as high as 1000 K. The reason being that, unlike monoolefin + OH reactions, addition of OH radicals to these conjugated diolefins preferentially yield resonantly stabilized adduct radicals that land into a deeper well (see reference [13] and references cited therein). The resulting stabilized radicals can now live longer, thereby opening up new channels at lower temperatures. These resonantly stabilized adduct radicals react slowly with molecular oxygen which suppresses the low-temperature combustion behaviour of these conjugated dioelfins. Nontheless, hydrogen abstraction reactions prevail for these dienes + OH reactions at high temperatures, and their role becomes increasingly important if sp^2 carbon atoms are replaced with sp^3 and/or conjugation is broken by inserting sp^3 hybridized carbon atoms in the (poly)olefin molecular skeleton. This is seen when one compares the overall rate coeficients for OH radical reactions with 1-pentene and

1,3-pentadiene. As seen in Figure 2, 1-pentene reacts faster than 1,3-pentadiene, indicating that H-abstraction pathways are the main active routes at high temperatures. Among the olefins studied here, 1,4-pentadiene displays the highest reactivity towards OH radicals. This is probably not surprising because of the ease of hydrogen abstraction from the bis-allylic position. Due to super-resonance stabilization of the incipient radical, the abstraction pathway from the bis-allylic site is expected to be more kinetically and thermodynamically favorable as compared to the other abstraction pathways available for these olefins. The weak positive-temperature dependence and high reactiviy of 1,4-pentadiene with OH radicals points to small but sizable barrier height(s) for the abstraction and/or non-abstraction bimolecular pathway(s).

Low-Temperature Kinetics. We obtained low-temperature data for reactions R1-R4 in a flow reactor using laser flash photolysis and laser induced fluorescence (LPFR/LIF) technique over the temperature range of 291 to 468 K and pressure ~ 40 mbar. Figure 3 shows a typical LIF signal of OH radicals, as detected by the photomultiplier for a mixture of H_2O_2 and 2.81×10^{13} molecule cm^{-3} *cis*-1,3-pentadiene in helium; also shown is the OH-LIF signal for a control experiment carried out for a mixture of H_2O_2 and He only.

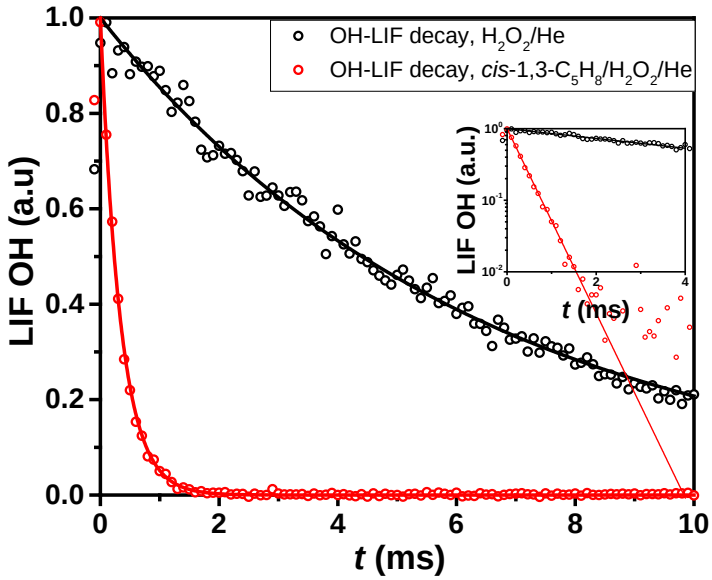

Figure 3: Red symbols show a typical OH-LIF decay time profile measured during OH + *cis*-1,3-pentadiene reaction (R2) at 323 K and 48 mbar using LPFR/LIF technique; black symbols represent OH-LIF decay time profile recorded in a control experiment.

As can be seen in Fig. 3, OH-LIF signal decays following first-order kinetics, i.e., ln[OH] vs time plot yields a straight line with a slope (k_{psuedo})= k_{bi} [Fuel]. The bimolecular rate constant (k_{bi}) can be readily obtained by dividing the slope with the fuel concentration. Alternatively, the bimolecular rate coefficient (k_{bi}) may also be obtained from the slope of OH-LIF singal as a function of fuel concentration as illustrated in Fig. 4 for *cis*-1,3-pentadiene + OH reaction. The slope of each straight line represents the rate coefficient of the target reaction at the corresponding temperature. The intercept of this plot represents the OH decay arising mostly from the reaction of OH radicals with the precursor H_2O_2 as well as diffusion out of the observation volume. Secondary chemistry, such as OH + OH = H_2O_2 play a minor role.

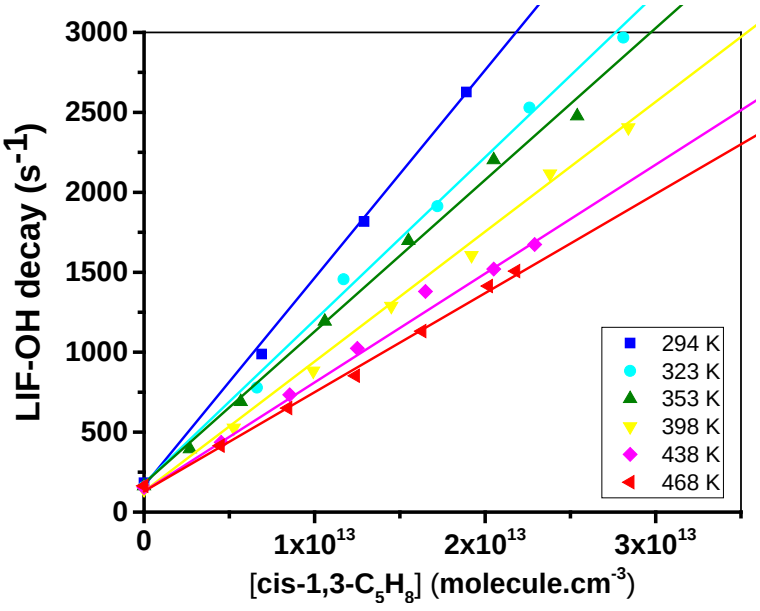

Figure 4: A typical plot for OH-LIF decay constant as a function of cis-1,3-pentadiene concentration. The slope of each line corresponds to the overall rate coefficient of OH + cis-1,3-pentadiene at the given temperature.

In a similar manner, the rate coefficients for OH reactions with other diolefins, 1,3-butadiene, *trans*-1,3-pentadiene and 1,4- pentadienes, were obtained. Table 3 compiles the measured overall rate coefficients at low temperatures. Figure 2 compares measured rate coefficients with the available literature data for 1,3-butadiene, *cis*-/*trans*-pentadiene, and 1,4-pentadiene. As explained earlier for high-temperature measurements, we adopted similar methodology to quantify uncertainties for the measured data at low temperatures. Table 4 summarizes the error sources and resulting uncertainties in our measured overall rate coefficients which were found to be 7% ,11%, 8% and 7% for R1, R2, R3 and R4, respectively.

Table 3: Overall low-temperature rate coefficients (p ~ 48 mbar) for OH reactions with 1,3-butadiene (R1), *cis*-1,3-pentadiene (R2), *trans*-1,3-pentadiene (R3) and 1,4-pentadiene (R4). See Table 4 for uncertainty in the measured rate coefficients.

***T*(K)**	**k_1 to k_4 (10^{-11}cm^3 molecule^{-1} s^{-1})**			
	1,3-butadiene	***cis*-1,3-pentadiene**	***trans*-1,3-pentadiene**	**1,4-pentadiene**
294 K	7.96	13.0	14.7	5.92
323 K	6.83	10.2	13.1	5.13
353 K	6.03	9.49	10.8	4.492
398 K	5.51	8.12	9.11	3.77
438 K	4.86	6.81	7.53	--
468 K	--	6.20	6.13	3.22

Table 4: Uncertainty quantification of low-temperature rate coefficients for OH reactions with 1,3-butadiene (R1), *cis*-1,3-pentadiene (R2), *trans*-1,3-pentadiene (R3) and 1,4-pentadiene (R4).

Uncertainty source	**Uncertainty bounds**				**Uncertainty to k_1-k_4**			
	1,3-butadiene	*cis*-1,3-pentadiene	*trans*-1,3-pentadiene	1,4-pentadiene	1,3-butadiene	*cis*-1,3-pentadiene	*trans*-1,3-pentadiene	1,4-pentadiene
Temperature	±10 K				0.3%			
Impurity (%)	±1%	±11%	±5%	±1%	0.2%	8%	5%	0.2%
Fuel concentration (%)	±5%				1%			

Fitting procedure	5%			5%		
LIF signal noise	1%			0.2%		
Other (pressure, impurities,…)				3%		
Root mean square error		7%	11%	8%	7%	

At low temperatures, it is generally accepted that olefins + OH reactions undergo almost exclusively via addition channel(s). With some exceptions, e.g., OH reactions with α-terpinene and α-phelandrene, hydrogen abstraction reactions contribute negligibly small (< 10%) to the total rate coefficients of OH + olefins, i.e., $k_{overall}$ (T) = $k_{addition}$ (T) + $k_{abstraction}$(T) ≈ $k_{addition}$(T).[23] This means one can simply estimate the overall rate coefficients by summing up the individual rate constants of OH addition to the specific double bond. The more sites an olefin can offer to incoming OH radicals for addition, the more reactive the olefin is. More importantly, their reactivity depends on the type of adduct radical being formed, i.e., primary, secondary, tertiary, or resonantly stabilized.[23] The extent of the stability of the adduct radical will determine the properties of the inner transition states in the potential energy surface of these (poly)olefins + OH reactions and, consequently, the reactivity of these (poly)olefins at low temperatures. In the current case, OH addition to one of the outer carbon atoms of 1,3-pentadiene results into the formation of resonantly stabilized adducts ($OHCH_2C^{\bullet}HCH=CHCH_3$ or $CH_2=CHC^{\bullet}HCH(OH)CH_3$). Such resonantly stabilized adduct is not possible for OH addition in 1-pentene, and it offers only two carbon sites for OH addition. Although 1,3-pentadiene has four carbon sites for OH addition, OH preferentially goes to one of the outer carbon atoms to achieve resonance stabilization. This would explain why 1,3-pentadiene shows higher reactivity (~ 4 times) with OH radicals than 1-pentene. At low temperatures, in contrary to high temperatures,

cis- and *trans*- 1,3-pentadienes clearly showed an effect of steric hinderance by displaying differences in the reactivity (see Fig. 2). At 298 K, *cis*-conformer of 1,3 pentadiene exhibits ~20% reduction in the reactivity towards OH radicals which is not surprising considering that the OH radicals approaching from the syn side of 1,3-pentadiene skeleton gets partly hindered, and thus affecting the formation of the pre-reactive π-complex. At room temperature, we determined a rate coefficient of k_2 (~ 48 mbar) = 1.29×10^{-10} cm^3 s^{-1} for cis-1,3-pentadiene + OH reaction which matches very well with the values reported by Magneron et al.[20] k_2 (1 bar) = 1.21×10^{-10} cm^3 s^{-1}) and Ohta et al.[18] k_2 (30 mbar) = 1.02×10^{-10} cm^3 s^{-1}. This suggests that the measured rate coefficients (k_2) are close to the high-pressure limit. Similarly, our value of k_3 (~48 mbar, 294 K) = 1.47×10^{-10} cm^3 s^{-1} for *trans*-1,3-pentadiene + OH is in very good agreement with that of Magneron et al.[20] k_3 (1 bar, 298 K) = 1.30×10^{-10} cm^3 s^{-1}, revealing that our low-temperature measurements are also near the high-pressure limit for this isomer.

As seen in Fig. 2, our low-temperature measurements of 1,3-butadiene + OH reaction at ~ 48 mbar compare excellently with the values reported by Grosjean and Williams [21] (p ~1.3 mbar) and Atkinson et al. [22] (p ~67 mbar). Similar to 1,3-pentadiene + OH reaction, the reaction of 1,3-butadiene with OH radicals is close to the high-pressure limit even at a pressure as low as 1 mbar. 1,3-Butadeine + OH reaction exhibits slower reactivity, roughly by a factor of 2, as compared to both conformers of 1,3-pentadienes though these are conjugated dienes and the ensuing adduct radicals, after OH addition, are expected to give similar resonance stabilization due to the delocalization of the product radicals over three carbon atoms of the conjugated dienes. The enhanced reactivity of 1,3-pentadienes may be stemming from the additional contribution of allylic hydrogen abstraction which are absent in 1,3-butadiene. The abstraction of allylic hydrogens from 1,3-pentadiene results in the formation of product radical (CH_2=CH-

CH=CH-CH2$^{\bullet}$) that is super-resonantly stabilized. Such super-resonantly stabilized radicals (conjugated allyl) have a resonance energy of 80 kJ/mol, roughly 20 kJ/mol higher than non-conjugated allyl radical.[11] This extra stabilization in the product allyl radical enhances the hydrogen abstraction reactions of dienes with OH radicals, as seen previously for the reactions of OH radicals with α-terpinene and α-phelandrene.[47] The importance of abstraction reactions of conjugated diolefins to form super- resonance stabilized allylic radicals and their major share to the overall rate coefficients at room temperature have been reported in the literature.[23, 47]

In contrast to the high-temperature chemistry, we observed that at lower temperatures 1,4-pentadiene shows the slowest reactivity towards OH radicals among diolefins. Unlike 1,3-butadiene and 1,3-pentadiene, OH addition to the double bond of 1,4 pentadiene results in an adduct radical that lacks resonance stabilization. This lack of resonance stabilization of the product radical affects the reaction exogercity and the barrier height of the inner transition states forming the adduct radical which ultimately influence the overall reactivity of 1,4-pentadine with OH radicals. Unlike the case of addition reaction, the ensuing free radical after hydrogen abstraction at the bis-allylic site of 1,4-pentadiene by OH radicals is super-resonantly stabilized due to spreading of unpaired electron out to all five carbon atoms. A recent study has shown that the reaction kinetics of olefins + OH is greatly influenced by both the inner and outer transition states at low temperatures. Therefore, for 1,4,-pentadiene + OH reaction, addition complex does not seem to be as favored as that of 1,3-butadiene and 1,3-pentadiene + OH reactions. Instead, a significant reaction flux may proceed *via* abstraction of secondary allyl hydrogens which leads to the formation of super-resonantly stabilized secondary allyl radicals.

Our measured value for k_4 (~48 mbar, 294 K) = 5.92×10^{-11} cm^3 s^{-1} compares very well with that from Ohta et al.[18], k_4 (~1 bar, 298 K) = 5.06×10^{-11} cm^3 s^{-1}, and Atkinson et al.[49], k_4 (~1 bar, 298

K) = 5.30 $\times 10^{-11}$ cm^3 s^{-1}. Similar to the other dienes + OH reactions studied here, the reaction of 1,4-pentadiene with OH radicals displays negligible pressure dependence, indicating that the measured values of the rate coefficients are close to the high-pressure limit. Unlike conjugated diolefins + OH reactions where SAR predictions deliver excellent agreement (within 7% of the experimental values),[23] we observe SAR to be not performing as well for 1,4-pentadine + OH reaction, where the deviation is as large as 30%. Deviations of similar magnitude were also observed for the reactions of OH radicals with other dieolefins, e.g., 1,4-hexadiene, α-phenllandrene and α-terpinene. For these olefinic compounds, abstraction reactions are important and their contribution can be significant even at low temperatures. Therefore, SAR prediction by summation of site-specific rate coefficients for OH addition is not adequate for calculating the overall rate coefficients.

Under finite temperatures and pressures of our LPFR/LIF experiments, we did not observe any sign of back dissociation of the addition complex as the loss of OH radicals was purely mono-exponential in all cases. This may have two implications. (i) Conjugated olefins form more stable addition complexes with OH radicals as compared to the non-conjugated olefins, implying quasi-irreversible reaction for the conjugated olefins. In fact, resonantly-stabilized addition complex of 1,3-butadiene + OH lands into a well which is ~10 kcal/mol deeper as opposed to the non-resonance complex such as propene + OH.[13] (ii) It may also imply that the inner transiton states for the non-abstraction bimolecular channels, which are accessible under our experimental conditions, are submerged below the entrance channel. In either case, the net reaction may well be correlated with the capture rate cofficients. Like mono-olefins + OH reactions, low-temperature chemistry of diolefins + OH reactions is governed predominantly by addition reactions that typically display negative temperature dependence (see Fig. 2); however, the

severity depends on the properties of the outer and inner transiton states of these dienes + OH reactions.

4. Summary

Rate coefficients for the reaction of hydroxyl radicals with 1,3-butadiene (R1), *cis*- and *trans*-1.3-pentadiene (R2 and R3) and 1,4-pentadiene (R4) were measured over a wide range of conditions using two experimental facilities. The measured rate coefficients may be expressed by the following modified Arrhenius expressions (units of $cm^3 molecule^{-1} s^{-1}$):

1. OH + *trans*-1,3-butadiene → products (R1) (*T* = 881 - 1348 K and 291 – 468 K, *p* ~ 1 – 2.5 bar and *p* ~ 40 mbar).

$$k_1(T) = 3.65 \times 10^4\, T^{-5.16} \exp\left(-\frac{1310.8}{T}\right) + 2.49 \times 10^{-18}\, T^{2.33} \exp\left(-\frac{1850.3}{T}\right) \quad (1)$$

2. OH + *cis*-1,3-pentadiene → products (R2) (*T* = 881 - 1348 K and 291 – 468 K, *p* ~ 1 – 2.5 bar and *p* ~ 40 mbar).

$$k_2(T) = 5.43 \times 10^4\, T^{-5.16} \exp\left(-\frac{1295.8}{T}\right) + 3.18 \times 10^{-17}\, T^{2} \exp\left(-\frac{896.6}{T}\right) \quad (2)$$

3. OH + *trans*-1,3-pentadiene → products (R3) (*T* = 881 - 1348 K and 291 – 468 K, *p* ~ 1 – 2.5 bar and *p* ~ 40 mbar).

$$k_3(T) = 4.78 \times 10^4\, T^{-5.16} \exp\left(-\frac{1204.3}{T}\right) + 3.18 \times 10^{-17}\, T^{2} \exp\left(-\frac{896.6\ \mathrm{K}}{T}\right) \quad (3)$$

4. OH + 1,4-pentadiene → products (R4) (*T* = 881 - 1348 K and 291 – 468 K, *p* ~ 1 – 2.5 bar and *p* ~ 40 mbar).

$$k_4(T) = 2.65 \times 10^{-14}\, T^{0.86} \exp\left(\frac{808.3\ K}{T}\right) + 1.07 \times 10^{-19}\, T^{2.93} \exp\left(-\frac{3194.3\ \mathrm{K}}{T}\right) \quad (4)$$

Key findings from this work are summerized below :

- Diolefins + OH reactions display complex nature of temperature dependence due to various competing channels. Abstraction channels prevail at high temperatures, while these reactions

almost exclusively proceed *via* addition channels at low temperatures; some exceptions are encountered for 1,4-pentadiene + OH reaction.

- At low temperatures (T < 450 K), we observed that *trans*-1,3-pentadiene reacts faster than *cis*-1,3-pentadiene due to steric hinderance which impedes the incoming OH radicals to add to *cis*-1,3-pentadiene as opposed to *trans*-1,3-pentadiene. The steric effects are apparent for the differneces in the reactivity of stereo isomers.
- Conjugation in diolefins enhances reactivity towards OH radicals as compared to monoolefins at low temperatures, e.g., 1,3-*cis* or *trans*-pentadienes reacts four times faster than 1-pentene with OH radicals.
- Super-resonance stabilization of the allylic adduct radical was found to have a great effect on the reactivity of diolefins + OH reactions at low temperatures. Due to the super allyl resonance, 1,3-pentadiene + OH was found to react faster than 1,3-butadiene + OH, with additional contribution coming from the abstraction of allylic hydrogen atoms.
- At high temperatures, *cis* and *trans* isomers of 1,3-pentadiene were found to react at similar rates with OH radicals. At high temperatures, these diolefins + OH reactions undergo primarily *via* abstraction channels. At high temperatures, the reactivity trend of diolefins + OH reactions depends on the number and type of hydrogen atoms being abstracted, e.g., primary, secondary, tertiary, vinylic, allylic or super-allylic. Hydrogen abstraction from the allylic site of 1,3-pentadienes and 1,4-pentadiene becomes the major active channel at high temperatures, explaining the higher reactivity of these dienes with OH radicals than that of 1,3-butadiene.
- Addition and non-abstraction channels can make a significant share to the total rate coefficients even at 1000 K due to the resonance stabilization of the adduct radicals of conjugated diene + OH reactions.

- For the 1,4,-pentadiene + OH reaction, addition complex does not seem to be as favored as that of 1,3-butadiene and 1,3-pentadiene + OH reactions. Instead, a significant reaction flux may proceed *via* abstraction even at low temperatures.

Acknowledgements

Research reported in this work was funded by King Abdullah University of Science and Technology (KAUST). Work in Lille was funded by by the French ANR agency under contract No. ANR-11-LabX-0005-01 CaPPA (Chemical and Physical Properties of the Atmosphere) and the Région Hauts-de-France, the Ministère de l'Enseignement Supérieur et de la Recherche and the European Fund for Regional Economic Development (CPER Climibio).

References

1. OECD, *Oil 2018*. OECD Publishing, Paris, 2018; p 137.
2. Kalghatgi, G. T., The outlook for fuels for internal combustion engines. *International Journal of Engine Research* **2014,** *15* (4), 383-398.
3. Kalghatgi, G. T., Developments in internal combustion engines and implications for combustion science and future transport fuels. *Proceedings of the Combustion Institute* **2015,** *35* (1), 101-115.
4. Kalghatgi, G. T., *Fuel/engine interactions*. SAE International Warrendale, PA: 2014.
5. Sarathy, S. M.; Kukkadapu, G.; Mehl, M.; Javed, T.; Ahmed, A.; Naser, N.; Tekawade, A.; Kosiba, G.; AlAbbad, M.; Singh, E.; Park, S.; Rashidi, M. A.; Chung, S. H.; Roberts, W. L.; Oehlschlaeger, M. A.; Sung, C.-J.; Farooq, A., Compositional effects on the ignition of FACE gasolines. *Combustion and Flame* **2016,** *169*, 171-193.
6. Sarathy, S. M.; Kukkadapu, G.; Mehl, M.; Wang, W.; Javed, T.; Park, S.; Oehlschlaeger, M. A.; Farooq, A.; Pitz, W. J.; Sung, C.-J., Ignition of alkane-rich FACE gasoline fuels and their surrogate mixtures. *Proceedings of the Combustion Institute* **2015,** *35* (1), 249-257.
7. Energy, U. S. D. o. *Co-Optimization of Fuels and Engines*; 2016.
8. Westbrook, C. K.; Mehl, M.; Pitz, W. J.; Sjöberg, M., Chemical kinetics of octane sensitivity in a spark-ignition engine. *Combustion and Flame* **2017,** *175*, 2-15.
9. Leppard, W. R., The Chemical Origin of Fuel Octane Sensitivity. SAE International: 1990.
10. Westbrook, C. K.; Pitz, W. J.; Mehl, M.; Glaude, P.-A.; Herbinet, O.; Bax, S.; Battin-Leclerc, F.; Mathieu, O.; Petersen, E. L.; Bugler, J.; Curran, H. J., Experimental and Kinetic Modeling Study of 2-Methyl-2-Butene: Allylic Hydrocarbon Kinetics. *The Journal of Physical Chemistry A* **2015,** *119* (28), 7462-7480.
11. Senosiain, J. P.; Han, J. H.; Musgrave, C. B.; Golden, D. M., Use of quantum methods for a consistent approach to combustion modelling: Hydrocarbon bond dissociation energies. *Faraday Discuss.* **2002,** *119* (0), 173-189.
12. Puhan, S.; Saravanan, N.; Nagarajan, G.; Vedaraman, N., Effect of biodiesel unsaturated fatty acid on combustion characteristics of a DI compression ignition engine. *Biomass Bioenergy* **2010,** *34* (8), 1079-1088.
13. Vasu, S. S.; Zádor, J.; Davidson, D. F.; Hanson, R. K.; Golden, D. M.; Miller, J. A., High-Temperature Measurements and a Theoretical Study of the Reaction of OH with 1, 3-butadiene. *The Journal of Physical Chemistry A* **2010,** *114* (32), 8312-8318.
14. Vasu, S. S.; Huynh, L. K.; Davidson, D. F.; Hanson, R. K.; Golden, D. M., Reactions of OH with Butene Isomers: Measurements of the Overall Rates and a Theoretical Study. *J. Phys. Chem. A* **2011,** *115* (12), 2549-2556.
15. Khaled, F.; Badra, J.; Farooq, A., A shock tube study of C4–C6 straight chain alkenes+ OH reactions. *Proc. Combust.Inst* **2017,** *36* (1), 289-298.
16. Granata, S.; Faravelli, T.; Ranzi, E.; Olten, N.; Senkan, S., Kinetic modeling of counterflow diffusion flames of butadiene. *Combustion and Flame* **2002,** *131* (3), 273-284.
17. Goldaniga, A.; Faravelli, T.; Ranzi, E., The kinetic modeling of soot precursors in a butadiene flame. *Combustion and Flame* **2000,** *122* (3), 350-358.
18. Ohta, T., Rate constants for reactions of diolefins with hydroxyl radicals in the gas phase. Estimate of the rate constants from those for monoolefins. *The Journal of Physical Chemistry* **1983,** *87* (7), 1209-1213.
19. McGillen, M. R.; Percival, C. J.; Shallcross, D. E.; Harvey, J. N., Is hydrogen abstraction an important pathway in the reaction of alkenes with the OH radical? *Physical Chemistry Chemical Physics* **2007,** *9* (31), 4349-4356.

20. Magneron, I.; Mellouki, A.; Le Bras, G.; Moortgat, G.; Horowitz, A.; Wirtz, K., Photolysis and OH-initiated oxidation of glycolaldehyde under atmospheric conditions. *The Journal of Physical Chemistry A* **2005,** *109* (20), 4552-4561.
21. Grosjean, D.; Williams Ii, E. L., Environmental persistence of organic compounds estimated from structure-reactivity and linear free-energy relationships. Unsaturated aliphatics. *Atmospheric Environment. Part A. General Topics* **1992,** *26* (8), 1395-1405.
22. Atkinson, R.; Perry, R.; Pitts Jr, J., Absolute rate constants for the reaction of OH radicals with allene, 1, 3-butadiene, and 3-methyl-1-butene over the temperature range 299–424° K. *The Journal of Chemical Physics* **1977,** *67* (7), 3170-3174.
23. Peeters, J.; Boullart, W.; Pultau, V.; Vandenberk, S.; Vereecken, L., Structure−Activity Relationship for the Addition of OH to (Poly)alkenes: Site-Specific and Total Rate Constants. *The Journal of Physical Chemistry A* **2007,** *111* (9), 1618-1631.
24. D. King, M.; E. Canosa-Mas, C.; P. Wayne, R., A structure-activity relationship (SAR) for predicting rate constants for the reaction of NO3, OH and O3 with monoalkenes and conjugated dienes. *Physical Chemistry Chemical Physics* **1999,** *1* (9), 2239-2246.
25. Atkinson, R.; Arey, J., Atmospheric Degradation of Volatile Organic Compounds. *Chem. Rev.* **2003,** *103* (12), 4605-4638.
26. Li, Y.; O'Connor, E.; Zhou, C.-W.; Curran, H. J. In *An experimental study of butene isomers and 1, 3-butadiene ignition delay times at elevated pressures*, European Combustion Meeting, 2015.
27. Li, Y.; Klippenstein, S. J.; Zhou, C.-W.; Curran, H. J., Theoretical Kinetics Analysis for Ḣ Atom Addition to 1,3-Butadiene and Related Reactions on the Ċ4H7 Potential Energy Surface. *The Journal of Physical Chemistry A* **2017,** *121* (40), 7433-7445.
28. Li, Z.; Nguyen, P.; Fatima de Leon, M.; Wang, J. H.; Han, K.; He, G. Z., Experimental and Theoretical Study of Reaction of OH with 1,3-Butadiene. *The Journal of Physical Chemistry A* **2006,** *110* (8), 2698-2708.
29. Guenther, A.; Hewitt, C. N.; Erickson, D.; Fall, R.; Geron, C.; Graedel, T.; Harley, P.; Klinger, L.; Lerdau, M.; McKay, W., A global model of natural volatile organic compound emissions. *Journal of Geophysical Research: Atmospheres* **1995,** *100* (D5), 8873-8892.
30. Guenther, A.; Geron, C.; Pierce, T.; Lamb, B.; Harley, P.; Fall, R., Natural emissions of non-methane volatile organic compounds, carbon monoxide, and oxides of nitrogen from North America. *Atmos. Environ.* **2000,** *34* (12), 2205-2230.
31. Sawyer, R. F.; Harley, R. A.; Cadle, S. H.; Norbeck, J. M.; Slott, R.; Bravo, H. A., Mobile sources critical review: 1998 NARSTO assessment. *Atmos. Environ.* **2000,** *34* (12), 2161-2181.
32. Atkinson, R., A structure-activity relationship for the estimation of rate constants for the gas-phase reactions of OH radicals with organic compounds. *International Journal of Chemical Kinetics* **1987,** *19* (9), 799-828.
33. Kwok, E. S. C.; Atkinson, R., Estimation of hydroxyl radical reaction rate constants for gas-phase organic compounds using a structure-reactivity relationship: An update. *Atmos. Environ.* **1995,** *29* (14), 1685-1695.
34. Pfrang, C.; King, M. D.; Canosa-Mas, C. E.; Wayne, R. P., Structure–activity relations (SARs) for gas-phase reactions of NO3, OH and O3 with alkenes: An update. *Atmos. Environ.* **2006,** *40* (6), 1180-1186.
35. Khaled, F.; Giri, B. R.; Szőri, M.; Viskolcz, B.; Farooq, A., An experimental and theoretical study on the kinetic isotope effect of C2H6 and C2D6 reaction with OH. *Chemical Physics Letters* **2015,** *641*, 158-162.
36. Campbell, M. F.; Haylett, D. R.; Davidson, D. F.; Hanson, R. K., AEROFROSH: a shock condition calculator for multi-component fuel aerosol-laden flows. *Shock Waves* **2015**, 1-19.

37. Bradley, J., Shock waves in physics and chemistry. *Methuen, London* **1962**.
38. Benson, S. W.; O'Neal, H. E. *Kinetic data on gas phase unimolecular reactions*; DTIC Document: 1970.
39. Parker, A.; Jain, C.; Schoemaecker, C.; Fittschen, C., Kinetics of the reaction of OH radicals with CH3OH and CD3OD studied by laser photolysis coupled to high repetition rate laser induced fluorescence. *React. Kinet. Catal. Lett.* **2009,** *96* (2), 291-297.
40. Assaf, E.; Fittschen, C., Cross Section of OH Radical Overtone Transition near 7028 cm–1 and Measurement of the Rate Constant of the Reaction of OH with HO2 Radicals. *The Journal of Physical Chemistry A* **2016,** *120* (36), 7051-7059.
41. Assaf, E.; Song, B.; Tomas, A.; Schoemaecker, C.; Fittschen, C., Rate Constant of the Reaction between CH3O2 Radicals and OH Radicals revisited. *The Journal of Physical Chemistry A* **2016,** *120* (45), 8923-8932.
42. Pang, G. A.; Hanson, R. K.; Golden, D. M.; Bowman, C. T., High-Temperature Measurements of the Rate Constants for Reactions of OH with a Series of Large Normal Alkanes: n-Pentane, n-Heptane, and n-Nonane. *Z. Phys. Chem.* **2011,** *225* (11-12), 1157-1178.
43. Badra, J.; Elwardany, A. E.; Khaled, F.; Vasu, S. S.; Farooq, A., A shock tube and laser absorption study of ignition delay times and OH reaction rates of ketones: 2-Butanone and 3-buten-2-one. *Combustion and Flame* **2014,** *161* (3), 725-734.
44. Mehl, M.; Pitz, W. J.; Westbrook, C. K.; Curran, H. J., Kinetic modeling of gasoline surrogate components and mixtures under engine conditions. *Proceedings of the Combustion Institute* **2011,** *33* (1), 193-200.
45. Giri, B. R.; Szori, M.; Liu, D.; Khalid, F.; Mai, T. V.-T.; Huynh, L. K.; Viskolcz, B.; Farooq, A., An Experimental and Theoretical Kinetic Study of the Reaction of Hydroxyl Radicals with 1,4-Pentadiene. *Journal of Chemical Theory and Computation* **2018**.
46. Marley, W. M.; Jeffers, P. M., Shock tube cis-trans isomerization studies. IV. *The Journal of Physical Chemistry* **1975,** *79* (20), 2085-2087.
47. Vereecken, L.; Peeters, J., H-atom abstraction by OH-radicals from (biogenic) (poly)alkenes: C–H bond strengths and abstraction rates. *Chemical Physics Letters* **2001,** *333* (1–2), 162-168.
48. Zádor, J.; Jasper, A. W.; Miller, J. A., The reaction between propene and hydroxyl. *Phys. Chem. Chem. Phys.* **2009,** *11* (46), 11040-11053.
49. Atkinson, R., Gas-Phase Tropospheric Chemistry of Volatile Organic Compounds: 1. Alkanes and Alkenes. *Journal of Physical and Chemical Reference Data* **1997,** *26* (2), 215-290.